Modelling and Performance Evaluation of IDMT Overcurrent Relay Coordination for Fault Mitigation in the Nigerian 330-kV Transmission Network

Iniobong Essien[1], Iniobong Abasi-obot[1], Imo Nkan[1], Edidiong Ambrose[2], Etimbuk Abraham[3]

1. *Department of Electrical and Electronic Engineering, Faculty of Engineering, Akwa Ibom State University, Nigeria.*
2. *Department of Civil Engineering, Faculty of Engineering, Akwa Ibom State University, Nigeria.*
3. *Department of Electrical and Electronic Engineering, Faculty of Engineering, Topfaith University, Mkpatak, Nigeria.*

Abstract

Transmission-line faults can damage equipment and widen service interruptions when overcurrent protection is slow or non-selective. This study evaluates an Inverse Definite Minimum Time (IDMT) overcurrent-relay model on a MATLAB/Simulink representation of the Nigerian 330-kV, 28-bus transmission network, using the Afam Generating Station to Alaoji Transmission Substation corridor as the protection case. The model combines Root Mean Square (RMS) current measurement, current-transformer scaling, pickup comparison, Plug Setting Multiplier (PSM) calculation, inverse-time timing and a high-set logic branch. Fault simulations were performed with the Time Multiplier Setting (TMS) varied from 0.1 to 1.0. For the 0.001 ohm fault case, the enabled high-set branch produced a simulated relay-element delay of about 0.03 s. With the high-set branch disabled, operating time increased from 0.1538 s at TMS 0.1 to 1.5380 s at TMS 1.0. At TMS 0.1, high-set operation reduced relay-element delay by 80.5% for the same simulated condition. A normalized 1 kA primary-current comparison produced 50.00 A secondary current for a 100/5 Current Transformer (CT) and 4.17 A for a 1200/5 CT. The results demonstrate the linked effects of CT scaling, pickup, TMS and high-set logic on relay response.

Keywords: IDMT overcurrent relay; relay coordination; fault mitigation; Nigerian 330-kV network; TMS; PSM; current transformer; MATLAB/Simulink.

1. Introduction

Transmission-line protection system must be coordinated in a way that it clears clear faults on the line quickly without disconnecting healthy parts of the network. This balance in speed, sensitivity and selectivity is especially important on long high-voltage corridors, where delayed clearing can increase thermal stress, depress voltage and increase the faulted area. A recent review of the Nigerian 330-kV transmission system identified relay coordination and timely fault isolation as continuous protection concerns [1].

IDMT overcurrent relays remain useful because operating time falls as fault current rises, while pickup and the Time Multiplier Setting provide practical variables for grading primary and backup protection. Work on dual-setting relays shows that TMS and plug setting remain central when network fault levels change with operating mode [2].

Recent researches have sought shorter relay operating times without sacrificing coordination constraints. Meta-heuristic optimization combined with non-standard tripping characteristics have reduced operating time in microgrid studies [3]. Adaptive approaches have also been developed for distribution networks in which distributed generation changes short-circuit conditions [4].

Operating speed is only an aspect of protection performance. Thermal withstand, coordination interval, relay reach and the short-circuit current seen by each device determines whether a setting is acceptable. [5] incorporated thermal-stress limits into overcurrent-relay optimization. [6] likewise showed that directional overcurrent coordination is strongly influenced by network structure, system constraints and the chosen optimization technique and objective.

Changes in topology and generation can also make fixed settings unsuitable. Adaptive hybrid overcurrent protection has been evaluated for medium-voltage networks with high shares of distributed energy resources [7]. Coordinated fault detection has been reported for low-voltage DC microgrids [8], and recent works on inverter-based resources showed that changed fault-current patterns can alter directional overcurrent coordination requirements [9].

The Afam Generating Station to Alaoji Transmission Substation case differs from the cited studies in voltage level, network structure and protection objective. The analysis follows the relay current path from CT scaling and pickup through PSM, TMS and high-set logic, then relates these settings to the simulated operating time.

2. Related Work and Research Gap

The studies reviewed in this work, illustrated three recurring approaches to overcurrent protection. While some optimized time and plug settings under coordination constraints [2,3,5,6], others adapt relay settings as fault contribution changes with generation or network topology [4,7,9]. Another group combines rapid fault recognition with coordinated tripping logic [8].

Relay operating time depends on fault current, the selected characteristics, CT scaling, breaker performance and network topology. Timing results reported in the literature therefore differ because the test systems, fault levels and coordination objectives are not the same [2,3,5,6]. The cited works are used in this study to establish technical context, not as direct numerical comparators.

Other published works establish the principles of CT scaling, PSM calculation and relay coordination, this study applies those principles to the Afam to Alaoji corridor and evaluates the resulting relay timing.

Table 1. Recent studies used to benchmark the proposed protection approach

Reference	Protection setting	Main contribution	Use in this study
[2] Tiwari et al., 2022	Microgrid	Dual-setting overcurrent coordination for two operating modes	Supports TMS and plug-setting formulation
[3] Alasali et al., 2022	Microgrid	Optimization with nonstandard tripping characteristics	Provides operating-time context
[4] Uma et al., 2023	DG-integrated distribution network	Adaptive TMS and PSM using RBFNN	Supports condition-dependent settings
[5] Rojnić et al., 2023	Active distribution network	Coordination with thermal-stress constraints	Supports equipment-stress consideration
[6] Foqha et al., 2024	Directional OCR review	Comprehensive assessment of optimization techniques	Provides coordination context
[7] Banerjee et al., 2024	DER-rich medium-voltage grid	Adaptive hybrid overcurrent protection	Provides adaptive-setting context
[8] Bhalla and Bhalja, 2024	Low-voltage DC microgrid	Fault detection with relay coordination	Provides coordinated-logic context
[9] Li et al., 2025	IBR-rich radial distribution network	Multi-objective DOCR coordination	Supports fault-level sensitivity

The comparison in Table 1 shows how the selected references support the setting variables and the interpretation of relay operating time. Their voltage levels, fault currents, CT ratios and coordination constraints differ from those of the present simulation, so their numerical results are not transferred directly to the Afam to Alaoji case.

3. Materials and Methods

3.1 Test system and protection corridor

A 330-kV, 28-bus Nigerian transmission-network representation was implemented in MATLAB/Simulink R2021b. Published studies of the Nigerian 330-kV grid provide the network context for the model [1, 10]. The Afam Generating Station to Alaoji Transmission Substation connection forms the protection case. The simplified one-line representation in Figure 1 identifies the terminal buses, circuit breakers, relay locations and protected corridor used in the setting analysis. The timing results in Section 4 refer to the 0.001 ohm fault case applied to this corridor model.

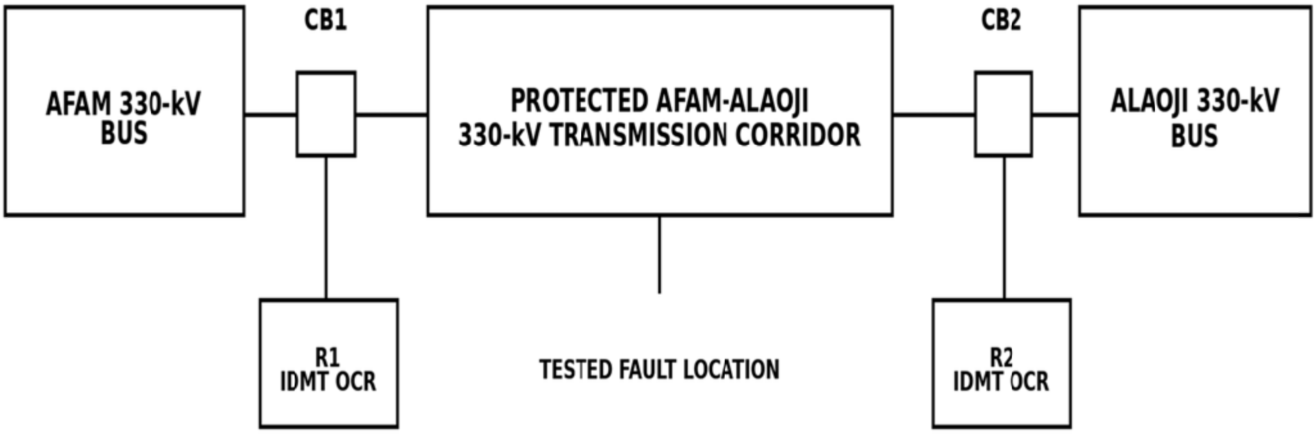

Figure 1. Simplified one-line representation of the Afam to Alaoji 330-kV protection case and relay locations

3.2 Relay settings and CT selection

CT ratio determines the secondary-current scale presented to the relay and therefore affects PSM. The sensitivity analysis compares 100/5 and 1200/5 ratios at the same normalized primary current. A 1200/5 ratio is used for the relay-input scaling study. CT selection in an operating installation also depends on load current, minimum and maximum short-circuit current, burden, accuracy class, saturation performance and relay requirements.

The parameters in Table 2 distinguish the CT-scaling comparison from the TMS timing sweep. When the high-set branch is active for the tested fault case, the simulated relay element operates after approximately 0.03 s. This is relay-element delay and does not include circuit-breaker opening time.

Table 2. Relay parameters used in the performance evaluation

Parameter	Value or range	Purpose
Nominal voltage	330 kV	Protected transmission corridor
Working CT ratio	1200/5	Working ratio for the normalized scaling study
CT secondary rating	5 A	Relay current input base
Fault resistance	0.001 ohm	Fault condition used for relay-behaviour test
TMS	0.1 to 1.0, step 0.1	Inverse-time timing sweep
High-set branch state	Enabled	High-set logic comparison
High-set branch state	Disabled	Isolates inverse-time response
High-set operating delay	Approximately 0.03 s	Simulated relay-logic delay after high-set operation

3.3 Research procedure

The procedure in Figure 2 begins with implementation of the 28-bus network representation in MATLAB/Simulink. Normal voltage and current are checked before the 0.001 ohm corridor fault case is applied. Relay-location RMS current is scaled by the selected CT ratio and compared with pickup to obtain PSM. Separate runs are performed with the high-set branch enabled and disabled. TMS is then varied from 0.1 to 1.0 and relay operating time is recorded.

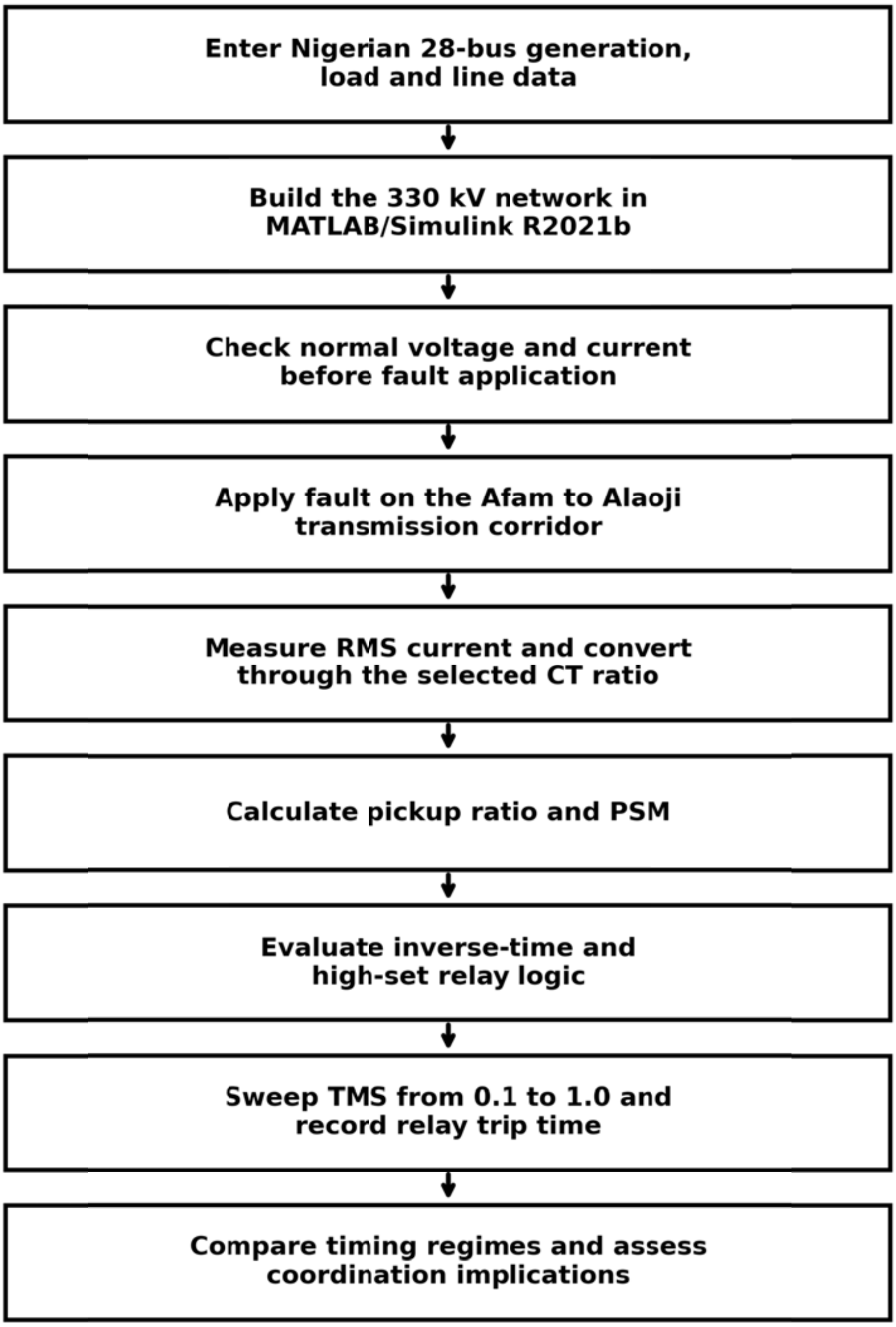

Figure 2. Research procedure used for the relay performance evaluation

3.4 Analytical model

Equation (1) converts primary RMS current to CT secondary current using the primary and secondary CT ratings.

$$I_{sec} = I_{pri} \times (I_{CT,sec} / I_{CT,pri}) \quad (1)$$

Equation (2) defines the Plug Setting Multiplier as the ratio of CT secondary current to relay pickup current.

$$\text{PSM} = I_{sec} / I_{pickup} \quad (2)$$

Equation (3) gives the generic inverse-time form used for IDMT interpretation. TMS scales operating time, while K, α and C define the selected characteristic [2,3,6,11]. Here, t_IDMT denotes relay operating time and PSM denotes the plug setting multiplier. The reported TMS sweep is a fixed-operating-point sensitivity test, so its operating-point coefficient is obtained directly from the simulated ratio t/TMS.

$$t_{IDMT} = (\text{K} \times \text{TMS}) / (\text{PSM}^{\alpha} - 1) + \text{C} \quad (3)$$

The characteristic families in Figure 3 show the expected reduction in relay operating time as PSM increases. IEC 60255-151 specifies functional requirements and time-delay characteristics for overcurrent protection, while the cited coordination studies provide application context [2,3,6,11].

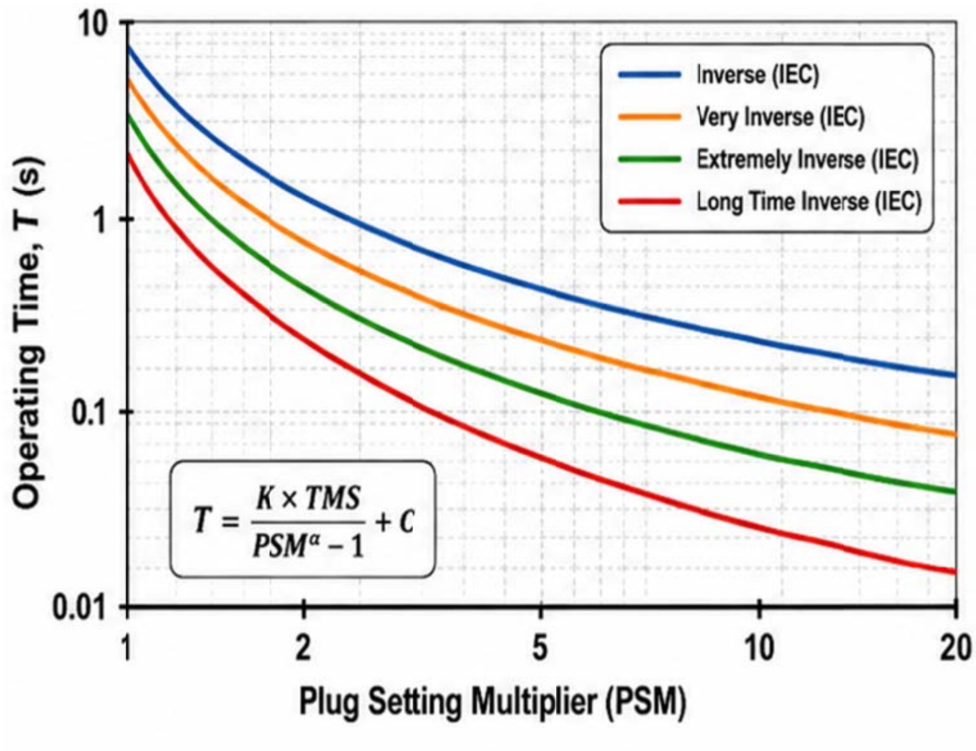

Figure 3. IDMT inverse-time characteristic curves used to interpret relay operating behaviour

Equation (4) summarizes the fixed-operating-point relationship observed in the TMS sweep. Across the reported data, K_op = t/TMS = 1.538 s [2,6,11].

$$t = K_{op} \times \text{TMS}, \quad K_{op} = 1.538\ \text{s} \qquad (4)$$

Equation (5) expresses the simulated high-set branch delay after the high-set condition has been satisfied. The reported relay-element delay is approximately 0.03 s; circuit-breaker opening time is not included.

$$t_{HS} \approx 0.03\ \text{s when PSM} \geq \text{PSM}_{HS} \qquad (5)$$

3.5 Relay decision logic and performance measures

The signal path in Figure 4 begins with three-phase currents, followed by 1200/5 CT scaling and RMS calculation. Pickup comparison produces PSM, which is passed to the inverse-time and high-set elements. The settings block supplies pickup, TMS and curve parameters to the relay logic. The decision sequence in Figure 5 checks pickup through PSM before selecting restrained operation, delayed IDMT operation or the high-set branch.

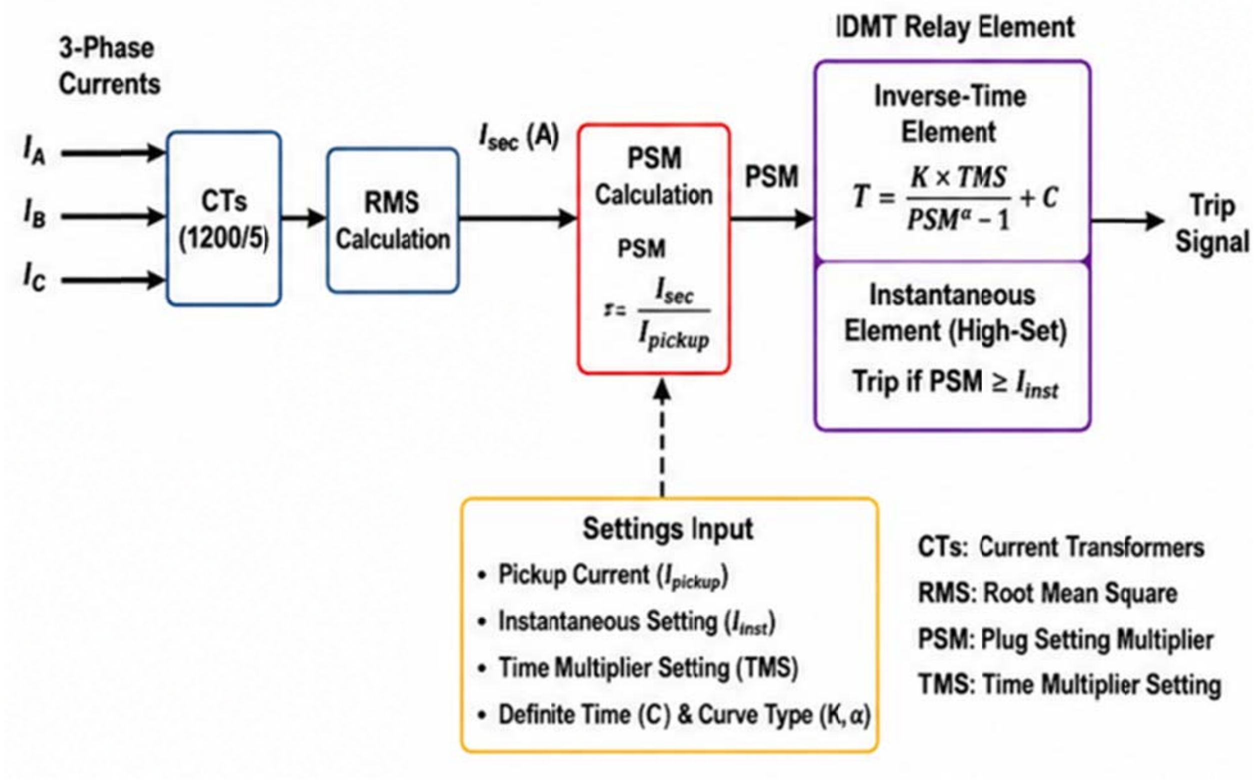

Figure 4. IDMT overcurrent-relay protection structure and setting inputs

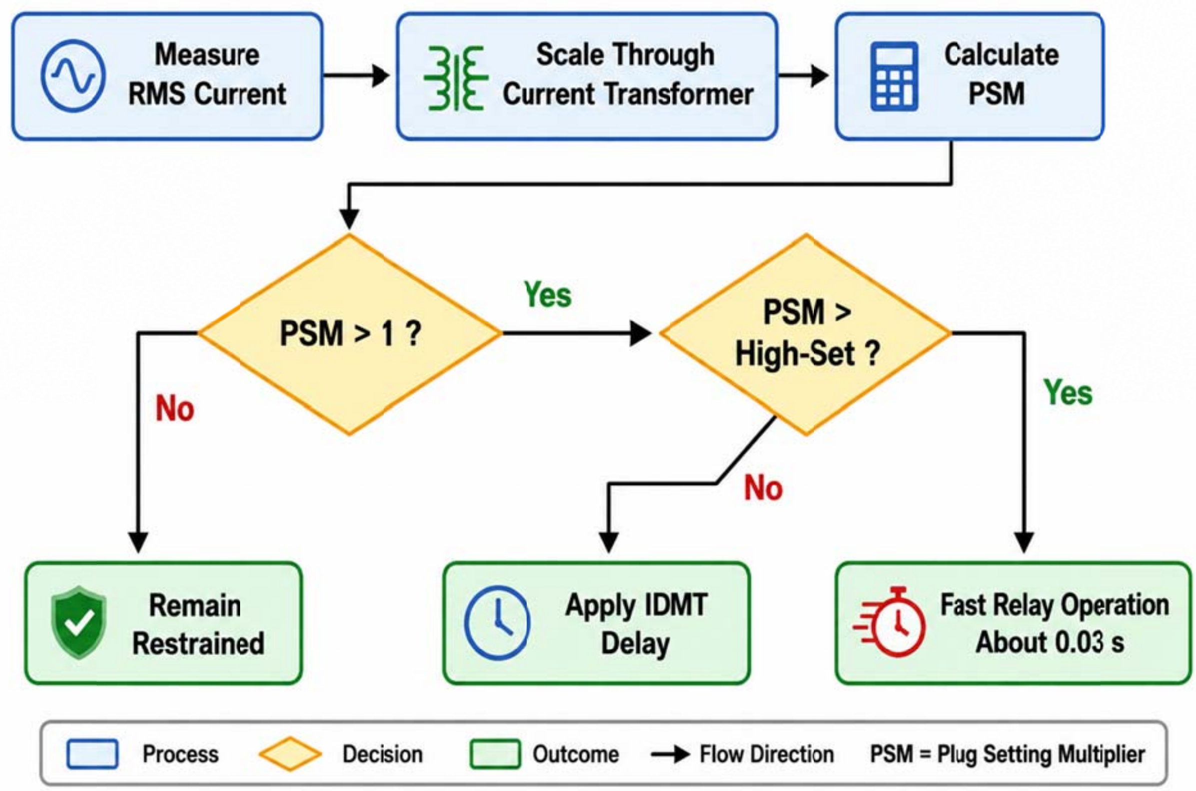

Figure 5. Decision logic of the simulated IDMT overcurrent relay

Equation (6) defines TMS timing sensitivity as the change in relay operating time divided by the corresponding change in time multiplier.

$$S_{TMS} = \Delta t \,/\, \Delta \mathrm{TMS} \quad (6)$$

4. Results

4.1 Relay operating time

Two timing regimes are evident in the simulation. For the 0.001 ohm corridor fault case, the enabled high-set branch gives a relay-element delay of about 0.03 s. With that branch disabled, inverse-time operating time rises with TMS. The simulated values are reported in Table 3 and plotted in Figure 6. The values in Table 3 show that inverse-time delay rises from 0.1538 s at TMS 0.1 to 1.5380 s at TMS 1.0. The ratio t/TMS remains approximately 1.538 s because PSM and the curve parameters are fixed during the sweep. Once the high-set condition is met, the relay follows the faster high-set branch instead of the inverse-time delay.

Table 3. Simulated relay operating time for the TMS and high-set cases

S/N	TMS	High-set disabled, t (s)	High-set branch state	High-set active, t (s)
1	0.1	0.1538	Enabled	0.03
2	0.2	0.3076	Enabled	0.03
3	0.3	0.4614	Enabled	0.03
4	0.4	0.6152	Enabled	0.03
5	0.5	0.7690	Enabled	0.03
6	0.6	0.9228	Enabled	0.03
7	0.7	1.0766	Enabled	0.03
8	0.8	1.2304	Enabled	0.03
9	0.9	1.3842	Enabled	0.03
10	1.0	1.5380	Enabled	0.03

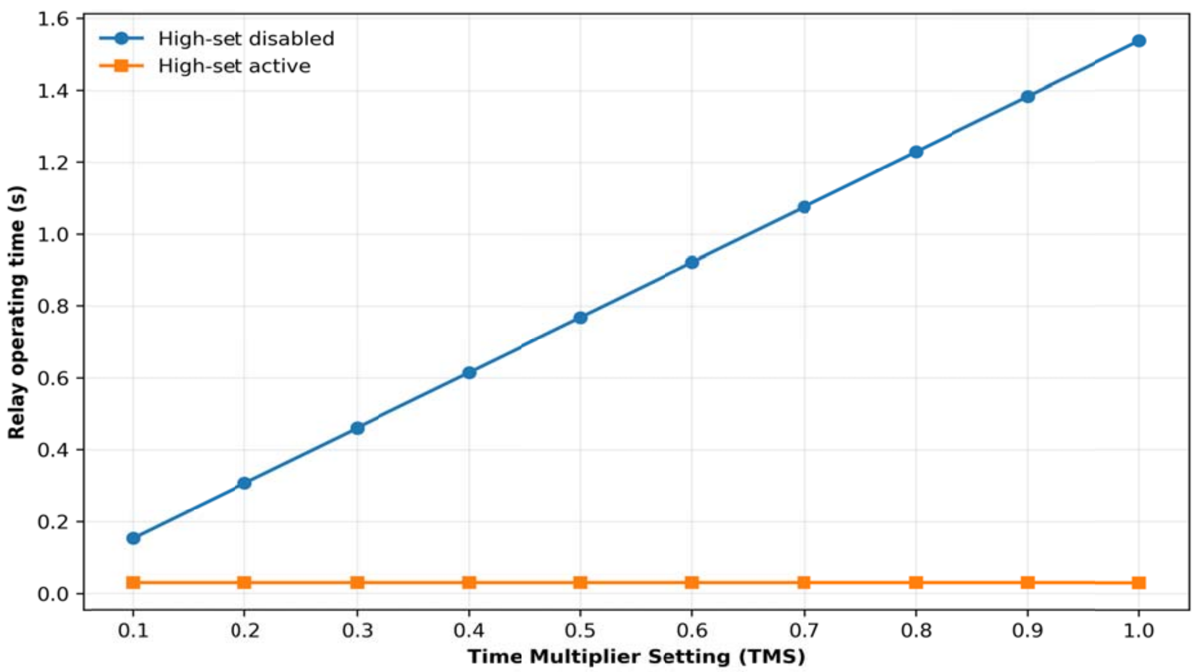

Figure 6. Relay operating time with the high-set element active and disabled

4.2 High-set timing advantage

High-set timing advantage was calculated from the simulated values in Table 3. The derived quantities in Table 4 are the absolute time saved, percentage reduction and inverse-time-to-high-set time ratio. The trend in Figure 7 shows how the absolute timing difference grows as the inverse-time delay increases. The values in Table 4 and Figure 7 show a time saving of 0.1238 s at TMS 0.1 and 1.5080 s at TMS 1.0. Relative to inverse-time operation, the corresponding relay-element reduction rises from 80.5% to 98.0%. These values refer to relay logic and exclude circuit-breaker opening time.

Table 4. Derived timing advantage of high-set operation relative to inverse-time operation

S/N	TMS	Inverse-time t (s)	High-set t (s)	Time saved (s)	Reduction (%)	Time ratio
1	0.1	0.1538	0.03	0.1238	80.5	5.1
2	0.2	0.3076	0.03	0.2776	90.2	10.3
3	0.3	0.4614	0.03	0.4314	93.5	15.4
4	0.4	0.6152	0.03	0.5852	95.1	20.5
5	0.5	0.7690	0.03	0.7390	96.1	25.6
6	0.6	0.9228	0.03	0.8928	96.7	30.8
7	0.7	1.0766	0.03	1.0466	97.2	35.9
8	0.8	1.2304	0.03	1.2004	97.6	41.0
9	0.9	1.3842	0.03	1.3542	97.8	46.1
10	1.0	1.5380	0.03	1.5080	98.0	51.3

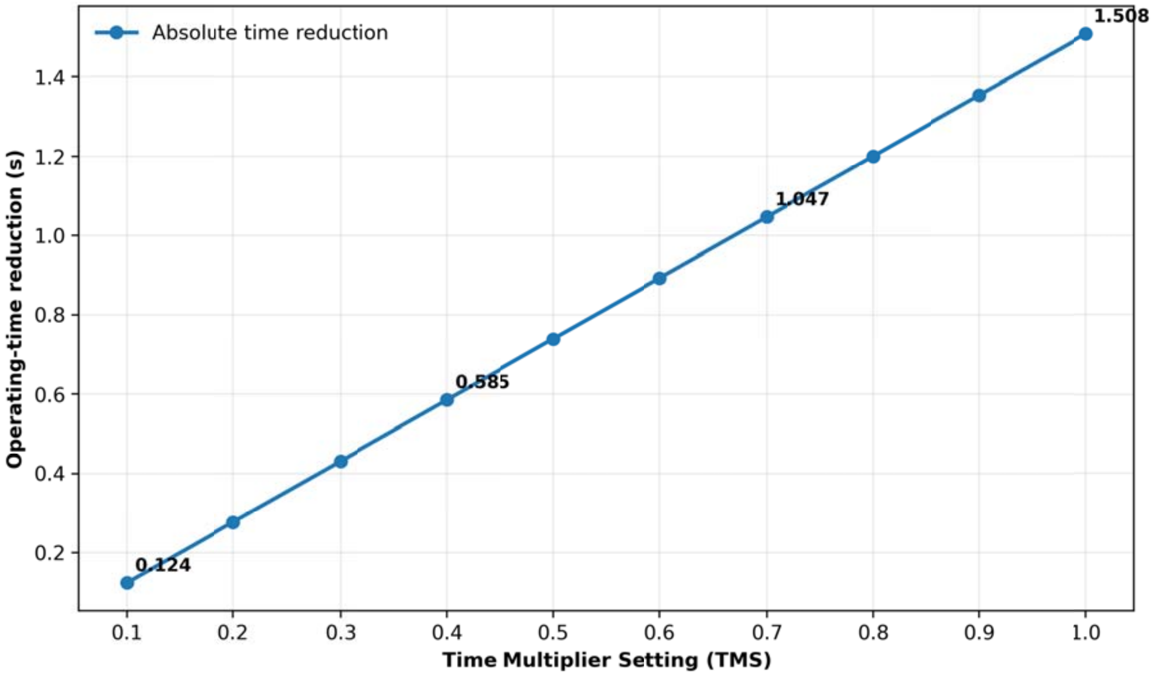

Figure 7. Absolute relay operating-time reduction produced by high-set operation

4.3 TMS proportionality and timing sensitivity

The normalized timing values in Table 5 and Figure 8 provide a direct check on the TMS sweep. Because the tested PSM and curve parameters are unchanged, both t/TMS and the incremental slope remain approximately 1.538 s per unit TMS. The constant value in Table 5 and the flat trend in Figure 8 confirm that TMS acts as a multiplicative timing factor at the tested operating point. This result is consistent with the fixed-operating-point form in Equation (4).

Table 5. TMS proportionality and incremental timing sensitivity

S/N	TMS	Inverse-time t (s)	t/TMS (s)	Incremental slope $\Delta t/\Delta TMS$
1	0.1	0.1538	1.538	N/A
2	0.2	0.3076	1.538	1.538
3	0.3	0.4614	1.538	1.538
4	0.4	0.6152	1.538	1.538
5	0.5	0.7690	1.538	1.538
6	0.6	0.9228	1.538	1.538

S/N	TMS	Inverse-time t (s)	t/TMS (s)	Incremental slope Δt/ΔTMS
7	0.7	1.0766	1.538	1.538
8	0.8	1.2304	1.538	1.538
9	0.9	1.3842	1.538	1.538
10	1.0	1.5380	1.538	1.538

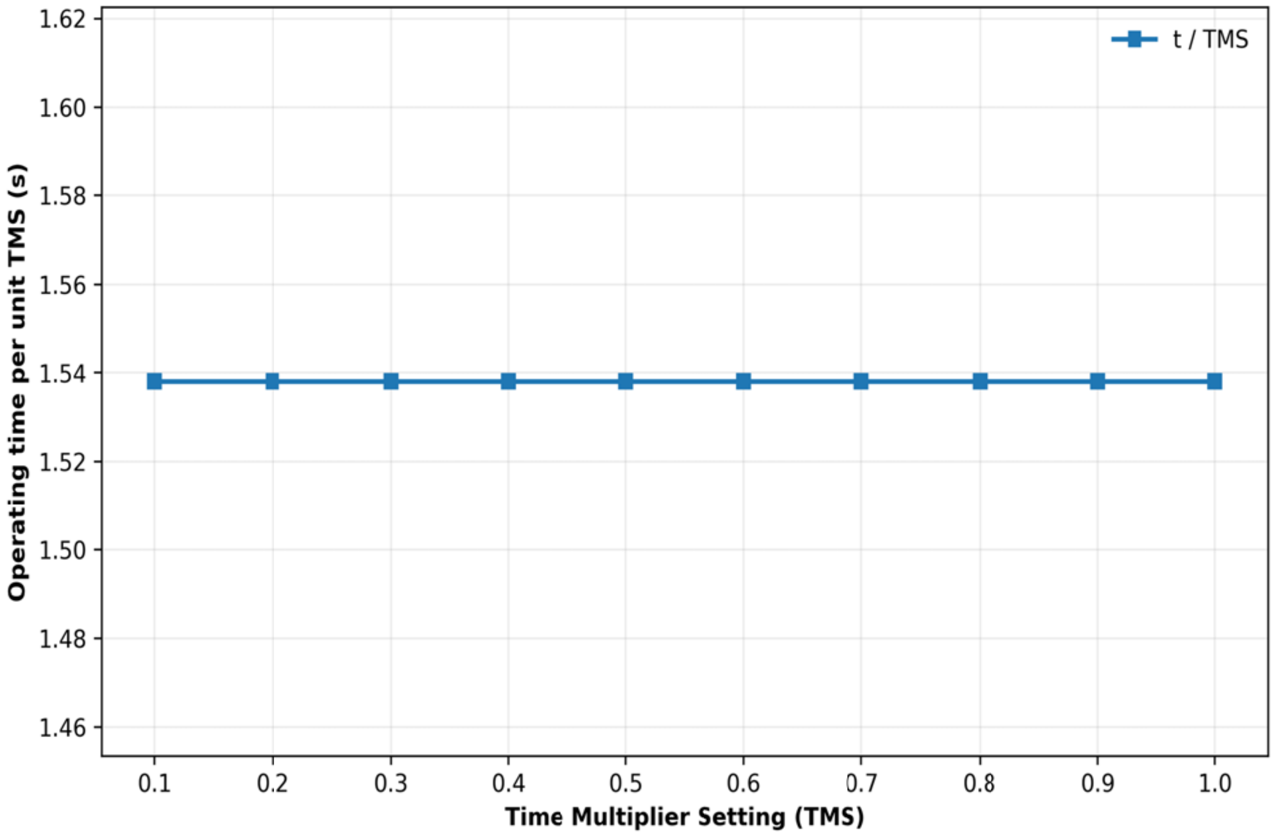

Figure 8. Normalized inverse-time operating time across the TMS sweep

4.4 Normalized CT scaling comparison

Equation (1) was used to compare CT scaling at a normalized primary current of 1 kA. Applying the same primary current to both ratios isolates the transformation effect. The secondary-current results are given in Table 6 and Figure 9. At a normalized primary current of 1 kA, Table 6 and Figure 9 give 50.00 A secondary current for a 100/5 CT and approximately 4.17 A for a 1200/5 CT. The change from 100/5 to 1200/5 therefore reduces the relay-current scale by 91.7%. With pickup held constant, the lower secondary current also reduces PSM, which changes the inverse-time operating point.

Table 6. Normalized CT secondary-current comparison at 1 kA primary current

CT ratio	Primary:secondary ratio	Secondary current (A)	Change vs 100/5	Protection implication
100/5	20:1	50.00	Baseline	Larger secondary-current scale
1200/5	240:1	4.17	91.7% lower	Smaller secondary-current scale

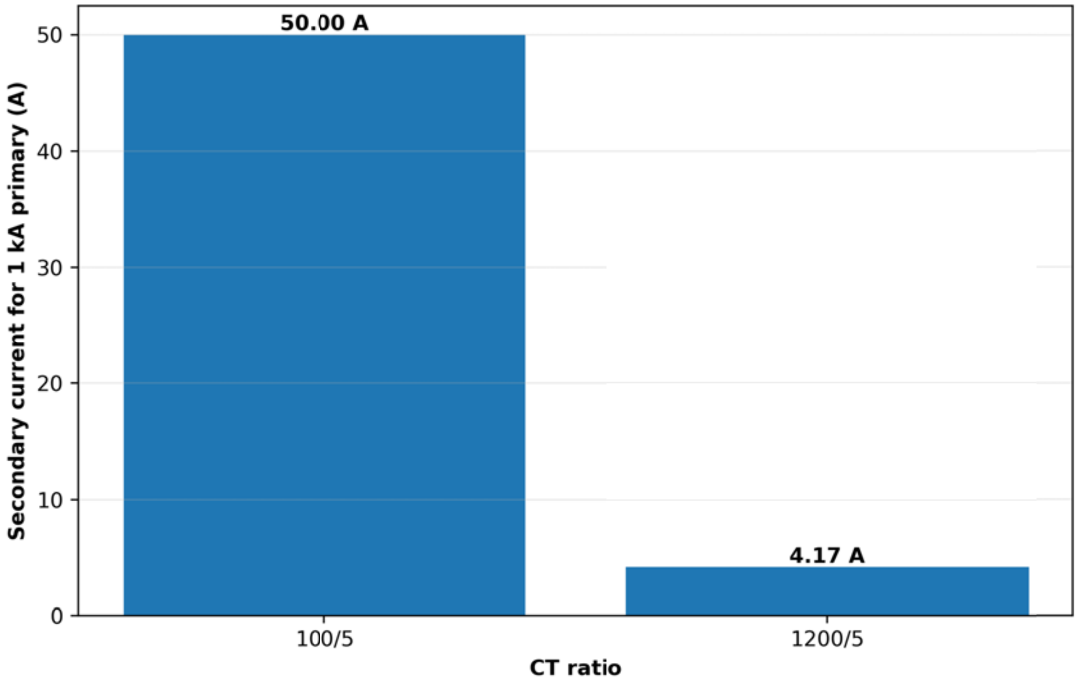

Figure 9. Normalized secondary current produced by the two CT ratios at 1 kA primary current

4.5 Comparison with published operating behaviour

The 0.03 s result is the simulated high-set branch delay, not the total fault-clearing time. Complete clearing also includes relay processing, coordination margin and circuit-breaker opening time. Published studies report primary-relay times in the order of tenths of a second for some systems, but their network data and relay characteristics differ from those used in the works of [2,3,5,6].

For the 0.001 ohm fault case, the high-set branch is 80.5% faster than the 0.1538 s inverse-time response at TMS 0.1. The comparison therefore quantifies the timing difference between the two relay branches under the same simulated condition.

4.6 Effect of CT ratio on PSM and relay behaviour

Changing the CT ratio changes the secondary current used to calculate PSM. Equation (1) shows that a larger CT primary rating produces a smaller secondary current for the same primary current; Equation (2) then gives a lower PSM when pickup is unchanged. The normalized CT test therefore isolates a setting interaction that must be considered alongside TMS.

Operational CT and relay settings are based on maximum load current, minimum and maximum short-circuit current, CT burden and accuracy class, saturation performance, pickup limits, line thermal rating and adjacent protection settings.

4.7 Coordination implications

Fast operation is useful only when selectivity is preserved. A high-set threshold that is set too low may operate for faults assigned to downstream protection, while excessive TMS prolongs thermal and voltage stress. Recent studies likewise treat relay time, pickup, grading interval and system condition as coupled coordination variables [2-7,9].

The Afam to Alaoji simulation characterizes the response of the tested relay logic at corridor level. Primary-backup grading applies the same setting principles to adjacent relays, short-circuit levels and circuit-breaker clearing times.

5. Discussion

The inverse-time and high-set branches produce distinctly different timing behaviour. TMS governs the delayed branch, whereas the high-set branch becomes dominant after its operating condition is met. Effective coordination therefore requires delayed grading and high-set selectivity to be considered together.

Changing the CT ratio from 100/5 to 1200/5 reduces the normalized relay-current scale by 91.7%. For an unchanged pickup, this reduction lowers PSM and shifts the inverse-time operating point. CT ratio and relay settings therefore cannot be selected independently.

For the tested fault case, the 0.03 s high-set branch shortens relay response after the high-set condition is satisfied. Selective clearing still depends on the chosen threshold, breaker operation and backup grading. The reported value therefore describes relay-element timing rather than complete substation clearing performance.

Field coordination combines corridor relay settings with primary-backup grading, utility short-circuit levels, breaker operating times and CT performance data.

5.1 Study scope

The study evaluates relay-element timing and CT scaling for the Afam to Alaoji corridor under the 0.001 ohm simulated fault case. Its results are limited to the corridor-level setting analysis represented by the available simulation outputs.

6. Practical Applications

6.1 Setting review for the Afam to Alaoji corridor

Protection Engineers can apply the workflow to the Afam to Alaoji corridor using approved fault-current studies, installed CT data, breaker clearing times and adjacent protection settings. The TMS sweep supports delayed-setting assessment, while a calibrated high-set test establishes instantaneous reach for the intended protection zone.

6.2 Pre-commissioning and maintenance testing

Secondary-injection testing can compare physical relay response with calculated PSM and expected operating time after field settings are entered. Differences between model and relay behaviour can then be traced to CT ratio, pickup, characteristics selection or device configuration. Hardware-in-the-loop testing provides a further validation stage by connecting a programmed IDMT relay to a real-time digital power-system model [12].

6.3 Protection audit after network reinforcement

Changes in generation, transformer capacity or line configuration alter the short-circuit current sent to the relay. Repeating the CT-scaling and timing calculations after network reinforcement can reveal whether an operating point has shifted between the inverse-time and high-set regions.

6.4 Path toward adaptive setting groups

Validated setting groups can be prepared for distinct network states from utility fault studies. Condition-aware selection then extends the fixed-setting analysis toward adaptive protection, consistent with recent work on distributed-generation and DER-rich networks [4,7,9].

7. Conclusion

An IDMT overcurrent-relay model was evaluated for the Afam Generating Station to Alaoji Transmission Substation protection case within a Nigerian 330-kV, 28-bus simulation. For the 0.001 ohm fault case, the high-set branch produced a relay-element delay of approximately 0.03 s. With the high-set branch disabled, inverse-time operating time increased from 0.1538 s at TMS 0.1 to 1.5380 s at TMS 1.0. At a normalized primary current of 1 kA, the 100/5 and 1200/5 CT ratios produced 50.00 A and 4.17 A secondary current, respectively. The findings show that CT scaling, pickup, PSM, TMS and high-set logic jointly determine relay response. The corridor-level analysis supports relay-setting review, secondary-injection planning and subsequent primary-backup coordination studies.

References

[1] V. N. Ogar, K. A. A. Gamage, and S. Hussain, "Protection for 330 kV transmission line and recommendation for Nigerian transmission system: a review," International Journal of Electrical and Computer Engineering, vol. 12, no. 3, pp. 3320-3334, 2022, doi: 10.11591/ijece.v12i3.pp3320-3334.

[2] R. Tiwari, R. K. Singh, and N. K. Choudhary, "Coordination of dual setting overcurrent relays in microgrid with optimally determined relay characteristics for dual operating modes," Protection and Control of Modern Power Systems, vol. 7, art. 6, 2022, doi: 10.1186/s41601-022-00226-1.

[3] F. Alasali, E. Zarour, W. Holderbaum, and K. N. Nusair, "Highly fast innovative overcurrent protection scheme for microgrid using metaheuristic optimization algorithms and nonstandard tripping characteristics," IEEE Access, vol. 10, pp. 42208-42231, 2022, doi: 10.1109/ACCESS.2022.3168158.

[4] U. U. Uma, D. Nmadu, N. Ugwuanyi, O. E. Ogah, N. Eli-Chukwu, M. Eheduru, and A. Ekwue, "Adaptive overcurrent protection scheme coordination in presence of distributed generation using radial basis neural network," Protection and Control of Modern Power Systems, vol. 8, art. 63, 2023, doi: 10.1186/s41601-023-00336-4.

[5] M. Rojnić, R. Prenc, D. Topić, and I. Strnad, "A new methodology for optimization of overcurrent protection relays in active distribution networks regarding thermal stress curves," International Journal of Electrical Power & Energy Systems, vol. 152, art. 109216, 2023, doi: 10.1016/j.ijepes.2023.109216.

[6] T. Foqha, S. Alsadi, O. Omari, and S. S. Refaat, "Optimization techniques for directional overcurrent relay coordination: A comprehensive review," IEEE Access, vol. 12, pp. 1952-2006, 2024, doi: 10.1109/ACCESS.2023.3347393.

[7] G. Banerjee, C. Hachmann, J. Lipphardt, N. Wiese, and M. Braun, "Adaptive hybrid overcurrent protection scheme with high shares of distributed energy resources," Energies, vol. 17, no. 24, art. 6422, 2024, doi: 10.3390/en17246422.

[8] A. Bhalla and B. R. Bhalja, "A new fault detection and relay coordination technique for low voltage DC microgrid," Electric Power Systems Research, vol. 236, art. 110907, 2024, doi: 10.1016/j.epsr.2024.110907.

[9] J. Li, J. Feng, M. Huang, S. Liu, and G. Wang, "Optimal protection coordination for directional overcurrent relays in radial distribution networks with inverter-based distributed energy resources," International Journal of Electrical Power & Energy Systems, vol. 167, art. 110622, 2025, doi: 10.1016/j.ijepes.2025.110622.

[10] I. O. Akwukwaegbu, "Voltage instability investigation of Nigeria 330kV power network using continuation method," 2017 IEEE 3rd International Conference on Electro-Technology for National Development (NIGERCON), Owerri, Nigeria, 2017, doi: 10.1109/NIGERCON.2017.8281974.

[11] International Electrotechnical Commission, IEC 60255-151:2009, Measuring relays and protection equipment - Part 151: Functional requirements for over/under current protection. Geneva, Switzerland: IEC, 2009.

[12] G. Yadav, Y. Liao, and A. D. Burfield, "Hardware-in-the-loop testing for protective relays using real time digital simulator (RTDS)," Energies, vol. 16, no. 3, art. 1039, 2023, doi: 10.3390/en16031039.